AGU100 ADVANCING EARTH AND SPACE SCIENCE

Geophysical Research Letters

RESEARCH LETTER
10.1029/2018GL077594

Key Points:
- Bands and groove lanes on Europa and Ganymede form within a spectrum of morphologies controlled by lithosphere strength
- "Fossilized" ocean material accreted to the base of the ice shell may be exposed at the surface after high strain, notably in smooth bands
- Lithosphere thickness and cohesion loss are primary controls on the surface expression of tectonic deformation

Supporting Information:
- Supporting Information S1

Correspondence to:
S. M. Howell,
samuel.m.howell@jpl.nasa.gov

Citation:
Howell, S. M., & Pappalardo, R. T. (2018). Band formation and ocean-surface interaction on Europa and Ganymede. *Geophysical Research Letters*, *45*, 4701–4709. https://doi.org/10.1029/2018GL077594

Received 14 FEB 2018
Accepted 6 MAY 2018
Accepted article online 15 MAY 2018
Published online 28 MAY 2018
Corrected 9 JUL 2018

This article was corrected on 9 JUL 2018. See the end of the full text for details.

Band Formation and Ocean-Surface Interaction on Europa and Ganymede

Samuel M. Howell[1] **and Robert T. Pappalardo**[1]

[1]Jet Propulsion Laboratory, California Institute of Technology, Pasadena, CA, USA

Abstract Geologic activity in the outer H_2O ice shells of Europa and Ganymede, Galilean moons of Jupiter, may facilitate material exchange between global water oceans and the icy surface, fundamentally affecting potential habitability and the future search for life. Spacecraft imagery reveals surfaces rich with tectonic bands, predominantly attributed to the extension of brittle ice overlaying a convecting ice layer. However, the details of band-forming processes and links to potential ocean-surface exchange have remained elusive. We simulate ice shell faulting and convection with two-dimensional numerical models and track the movement of "fossil" ocean material frozen into the base of the ice shell and deformed through geologic time. We find that distinct band types form within a spectrum of extensional terrains correlated to lithosphere strength, governed by lithosphere thickness and cohesion. Furthermore, we find that smooth bands formed in weak lithosphere promote exposure of fossil ocean material at the surface.

Plain Language Summary The strength of rigid near-surface ice on Europa and Ganymede determines the terrains formed where the surface has pulled apart, and certain terrains can contain material originating in the subsurface ocean.

1. Introduction

Voyager and Galileo spacecraft images of Europa and Ganymede reveal the scars of tectonic activity imprinted in water ice shells tens of kilometers thick, inferred to overlay water oceans an order of magnitude deeper (Pappalardo et al., 1998; Prockter & Patterson, 2009; Spohn & Schubert, 2003). The origin and formation of these tectonized bands may be tied to processes that link the ice shell and the ocean, including spreading, rifting, subduction, and cryovolcanism (Head et al., 1999; Johnson et al., 2017; Kattenhorn & Prockter, 2014; Prockter & Patterson, 2009). Understanding these material exchange mechanisms is key to evaluating the potential habitability of ocean worlds (Grasset et al., 2013; Hand et al., 2009; Spohn & Schubert, 2003). For consistency, we use the term "band" to describe any tabular extensional zone of ridges and grooves that transects surrounding terrain, including the various band types on Europa and groove lanes (sulci) on Ganymede (Figure 1).

Tectonic bands are commonly tens of kilometers wide and hundreds of kilometers long, and they are inferred to occur where the brittle layer of the ice shell has diverged in response to tidal interaction with Jupiter (Pappalardo et al., 1998; Prockter & Patterson, 2009). These features are plentiful on the young surfaces of Europa (< ~60 Ma) and Ganymede (nominally ~2 Ga) (Zahnle et al., 2003), playing a primary role in ice shell resurfacing. Resurfacing at mid-ocean ridges on Earth serves as a potential analogue to band resurfacing (Prockter et al., 2002), where the igneous production and tectonic stretching of plate material accommodates the plate divergence.

Mid-ocean ridges have provided researchers with windows into the Earth's mantle, allowing tectonic features and chemistry observed at the crustal surface to improve our knowledge of the processes of melting and deformation occurring at depth. Studies that leverage numerical predictions of mid-ocean ridge evolution to interpret observed seafloor morphology have illuminated the processes of melting and deformation and identified key controls on seafloor morphology and faulting (e.g., Behn & Ito, 2008; Buck et al., 2005; Howell et al., 2016; Olive et al., 2015; Tian & Choi, 2017). Linking the wide range of observed band characteristics to numerical predictions of ice tectonics and flow can provide similar insight into properties of the ice shell interiors and ocean-surface exchange processes at Europa and Ganymede (Prockter et al., 2002).

Two-dimensional (2-D) modeling studies of Europa and Ganymede have contributed to our understanding of ice shell dynamics, including models of convection in the warm, ductile ice (asthenosphere) beneath the cold,

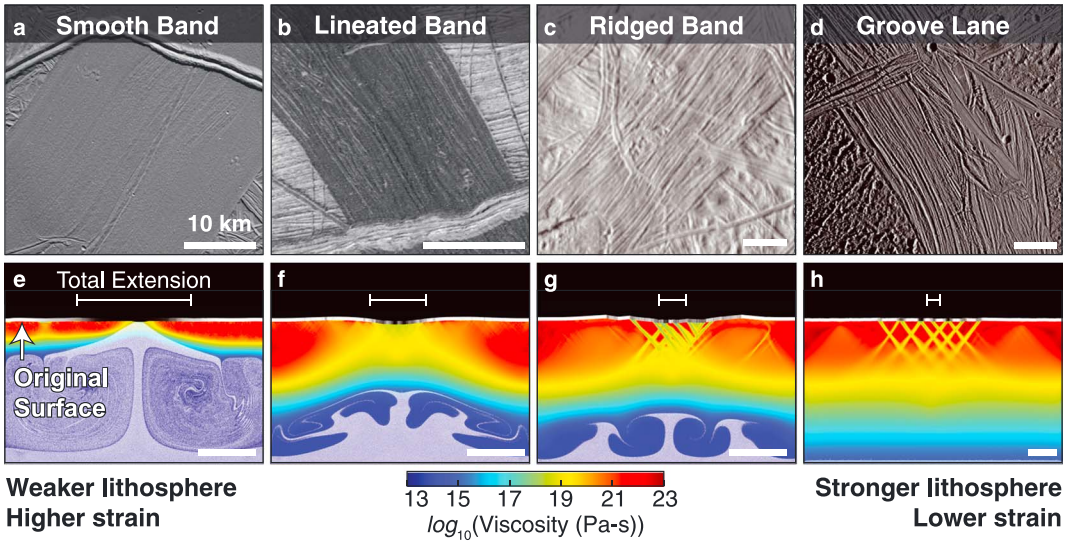

Figure 1. Galileo spacecraft images in map view showing band morphology (top row) and associated numerical models in cross section (bottom row). Images are of (a) Europa smooth band Thynia Linea, (b) Europa lineated band Yelland Linea, and (c) a ridged band in Europa's northern leading hemisphere, and (d) Ganymede groove lane Tiamat Sulcus. Selected models exhibit (e) symmetrical axial yielding with central axis for high regional strain, (f) variations in axial yielding that produce small-scale variations in surface ice exposure, (g) widespread asymmetrical faulting, and (h) large-scale rifting at low strain. Model outputs are colored by viscosity and show fossil ocean material (white dots within ductile ice). The model surfaces are colored white where the original surface has not been significantly disrupted and black where the model surface strain is the greatest and fresh interior ice is exposed.

brittle layer (lithosphere) for simplified rheologies (e.g., Mitri & Showman, 2005), and of melt migration beneath imposed tectonic features (Kalousová et al., 2016). However, few previous studies have modeled ice deformation that considers viscous flow, plastic yielding, elastic bending, and brittle failure for a full ice I rheology (Bland & McKinnon, 2015).

To explore band formation and ocean interaction in 2-D, we simulate viscoelastoplastic deformation in a solid ice I shell. Our models promote the spontaneous brittle localization of lithosphere failure onto shear bands that simulate faulting and track "fossil" ocean material that has frozen into the shell at the ice-water interface and subsequently deformed through geologic time. These simulations predict primary controls on band morphology and at which band types fossil ocean material may be exposed.

2. Geologic Setting

Studies based on Voyager and Galileo data have identified several extensional band morphological types. The relative albedo of these bands compared to their surroundings suggests that resurfacing has exposed native subsurface materials, generally darker than the older surface on Europa and brighter than the older surface on Ganymede (Pappalardo et al., 2004). It is debated whether and to what extent icy volcanism is involved in emplacement of Ganymede's grooved terrain (Pappalardo et al., 1998, 2004; Schenk et al., 2001), but volcanism is not considered in our modeling effort. In this study, we consider four prominent band types:

1. Smooth bands on Europa, for example, Thynia Linea (Figure 1a), are axially symmetric about a central trough and exhibit few apparent tectonic features. In surface maps, smooth bands can be "removed" at their margins to reconstruct the preexisting terrain with few gaps or overlaps (Prockter & Patterson, 2009). Such reconstruction reveals that bands commonly form within bounding ridges, inferred to correlate with preexisting weaknesses in the ice caused by prior tectonic deformation. The depth to which such weaknesses accommodate lithosphere separation remains unclear.
2. Lineated bands on Europa, for example, Yelland Linea (Figure 1b), exhibit tectonic lineations subparallel to a central trough and margins (Prockter & Patterson, 2009). The lineations, which may originate from faulting or fracture-related processes, are commonly axially symmetric and may show variation in trend along their length. Typically, reconstruction of lineated bands is possible, with at least one band margin originating as a preexisting ridge.

3. Ridged bands, such as an unnamed example in Europa's northern leading hemisphere (Figure 1c), exhibit ubiquitous surface modification, commonly without distinct margins (Prockter & Patterson, 2009). Their constituent ridges may be much longer and straighter than the features observed along lineated bands. Reconstruction is not possible, presumably because of modification or destruction of the previous surface through normal faulting, fracturing, or dike intrusion (Kattenhorn & Hurford, 2009).
4. Groove lanes on Ganymede, for example, Tiamat Sulcus (Figure 1d), contain subparallel faults that modify preexisting terrain over a broad zone (Pappalardo et al., 2004), analogous to lithosphere rifting processes on Earth (Pizzi et al., 2017). Because pervasive faulting has heavily deformed the original surface, reconstruction is impossible. Uncommonly, bands on Ganymede appear to be smooth without well-defined grooves.

3. Methods

Model calculations were carried out using the finite difference code SiStER (Simple Stokes solver with Exotic Rheologies), which has previously been applied to solve terrestrial tectonics problems (e.g., Olive et al., 2016). We extend SiStER to simulate the full rheology of ice I, including ductile flow, elastic bending, plastic yielding, and spontaneous brittle localization. The supporting information contains a full description of the numerical model, rheology (Goldsby & Kohlstedt, 2001), fault localization scheme, initial and boundary conditions, and tidal heating implementation.

Models are initialized with a conductive temperature profile from 95 K at the ice shell surface to 270 K at the base and include the temperature dependence of thermal conductivity (Nimmo & Manga, 2009). The simulated ice shell is pulled apart at the sides by setting the outflow velocity of the ice to 10 km/Myr (model strain rates of 1.4×10^{-14} to 2.8×10^{-14} s^{-1}), a plausible opening rate for Europan bands (Stempel et al., 2005).

To understand the influence of ice shell thickness on band morphology and evolution, we impose values relevant to both Europa ($H = 25$ km) and Ganymede ($H = 50$ km). Models are 300 elements wide × 200 elements deep (45 × 30 km, 150 m resolution for $H = 25$ km; and 90 × 60 km, 300 m resolution for $H = 50$ km). Because the thickness of the ice shell is predicted to be approximately uniform within a given region (Nimmo et al., 2003), we treat flat bottom boundary as an approximate water-ice solidus through which we track the inflow of new ice as fossil ocean material.

For each lithosphere thickness, we model three minimum viscosities at the melting temperature ($\eta_0 = 10^{13}$, 10^{14}, and 10^{15} Pa·s). Lower-viscosity models have a higher Rayleigh number and exhibit more vigorous convection, increasing heat flow through the ice shell and reducing the thickness of the cold lithosphere (e.g., Mitri & Showman, 2005). Furthermore, we impose a viscosity-dependent (thus temperature-dependent) tidal heat source consistent with Europa (Showman & Han, 2004); thus, models relevant to Ganymede have greater tidal heat dissipation than predicted in the current epoch. We assume that the heat flow into the ice shell from the core and tidal heating balances the heat flow out of the shell for each convective regime, so that ice shell thickness remains constant.

Finally, to understand how lithosphere cohesion affects band formation, we vary how easily faults form and accumulate damage in the lithosphere. Spontaneous brittle failure is accomplished by diminishing cohesion with increasing accumulated strain and restoring cohesion over a healing timescale, τ (Olive et al., 2016; Poliakov & Buck, 1998). As cohesion decreases, yield stress decreases, and the material deforms more easily into fault-like shear bands. Restoring cohesion over time forces less successful shear bands to "heal," and deformation focuses onto the remaining few large faults. For each η_0 and H, we model three brittle failure healing timescales (τ = 15 kyr, 300 kyr, and ∞).

We repeat two models ($H = 25$ km, $\eta_0 = 10^{13}$ and 10^{15} Pa·s, $\tau = 0$) with a horizontally centered cohesionless, frictionless column to simulate a preexisting weakness (e.g., a deep vertical fault beneath a Europa double ridge). The markers initiated within this column retain weakened material properties as they are advected through the model over time. Grid elements containing these markers have reduced yield strength and are more prone to plastic failure.

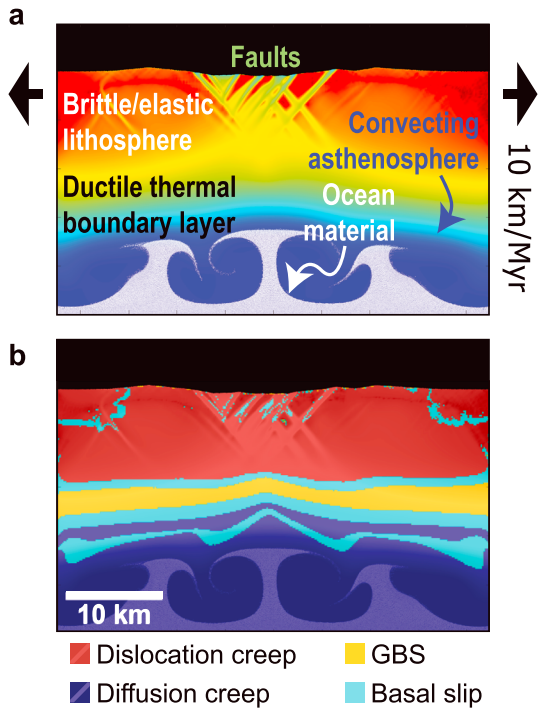

Figure 2. Annotated example model output. (a) Lithosphere faulting and asthenosphere convection (colors illustrate viscosity, as in Figure 1), and (b) dominant creep mechanisms (colors illustrate deformation mechanism).

4. Results and Discussion

4.1. General Model Trends

The temperature dependence of ice I produces a strong rheological lithosphere that exhibits brittle and elastic behavior, deforming primarily through dislocation creep and frictional plastic flow (Figure 2). Strain within the lithosphere may localize into narrow bands that resemble faults. Below the lithosphere, a ductile thermal boundary layer deforms through grain boundary sliding and basal slip. Finally, the warm, ductile rheological asthenosphere deforms through Newtonian diffusion creep.

The integrated lithosphere strength is greater when the lithosphere is thicker and the maximum yield stress at its base is therefore higher and when failure heals rapidly and localizes onto faults so that more of the lithosphere retains its cohesion. To demonstrate how changes in lithosphere strength affect band evolution for constant ice shell thickness, we present an illustrative spectrum of behaviors for four models with $H = 25$ km (Figure 3). These simulations differ in η_0, which controls the convective vigor of the asthenosphere and thus lithosphere thickness, and the fault healing timescale, τ, which affects fault localization.

As extension and vigorous convection thin the lithosphere at the band axis (Figure 3a), small, diffuse shear bands rapidly coalesce into a broad, plastically localized zone of yielding about a depressed central axis that exposes fresh surface ice. Reducing convective vigor by increasing η_0 results in a thicker lithosphere, delaying the formation of a broad plastic yielding zone (Figure 3b). Improving strain localization by imposing a cohesion recovery timescale, τ, causes the development of tightly grouped, discrete faults, rather than a smooth, broad yielding zone (Figure 3c). With a high viscosity and low τ, rifting occurs as faults disrupt a wide region at very low strains, rendering reconstruction impossible (Figure 3d). Because the faults form at low strains, the amount of fresh ice exposed along scarps is small. At strains greater than 25 km, the tectonically dominated lithosphere broadly yields and thins beneath the axis, producing a smooth band within the initial tectonized surface.

Because ice shell thickness remains fixed in our simulations, lithosphere advected out of the side boundaries must be replaced by influx of asthenosphere ice that cools and becomes rigid. Similarly, the asthenosphere must be replenished by accretion of new ice from the ocean. This accreted ice can be mixed into a vigorously convecting asthenosphere that ascends and cools to become new lithosphere. Deformation within the lithosphere is always well enough localized to allow the eventual exposure of entrained fossil ocean material at the surface.

We find that the thinnest lithosphere conveys fossil ocean material to the surface after tens of kilometers of extension and ~1 Myr, consistent with Europa band-opening widths and presumed lifespans (Stempel et al., 2005). For models that do not exhibit convection, fossil ocean material is exposed at the surface only after >2 Myr, beyond which the 40 km total model extension exceeds the width of most Europan bands (Prockter & Patterson, 2009).

4.2. Preexisting Weakness

Galileo spacecraft observations show that bands on Europa with few tectonic lineations tend to exhibit sharp margins that distinguish newly exposed dark ice from the surrounding bright terrain and that reconstruction of the preexisting terrain commonly reveals double ridges that preceded band formation (Figures 1a and 1b). However, the broad deformation predicted by our models (Figures 3a and 3b) is dispersed across tens of kilometers, with no clear boundary between the initial model surface and newly exposed ice. Thus, we test whether a preexisting vertical weakness will tend to promote formation of sharp margins for models of weak and strong lithosphere.

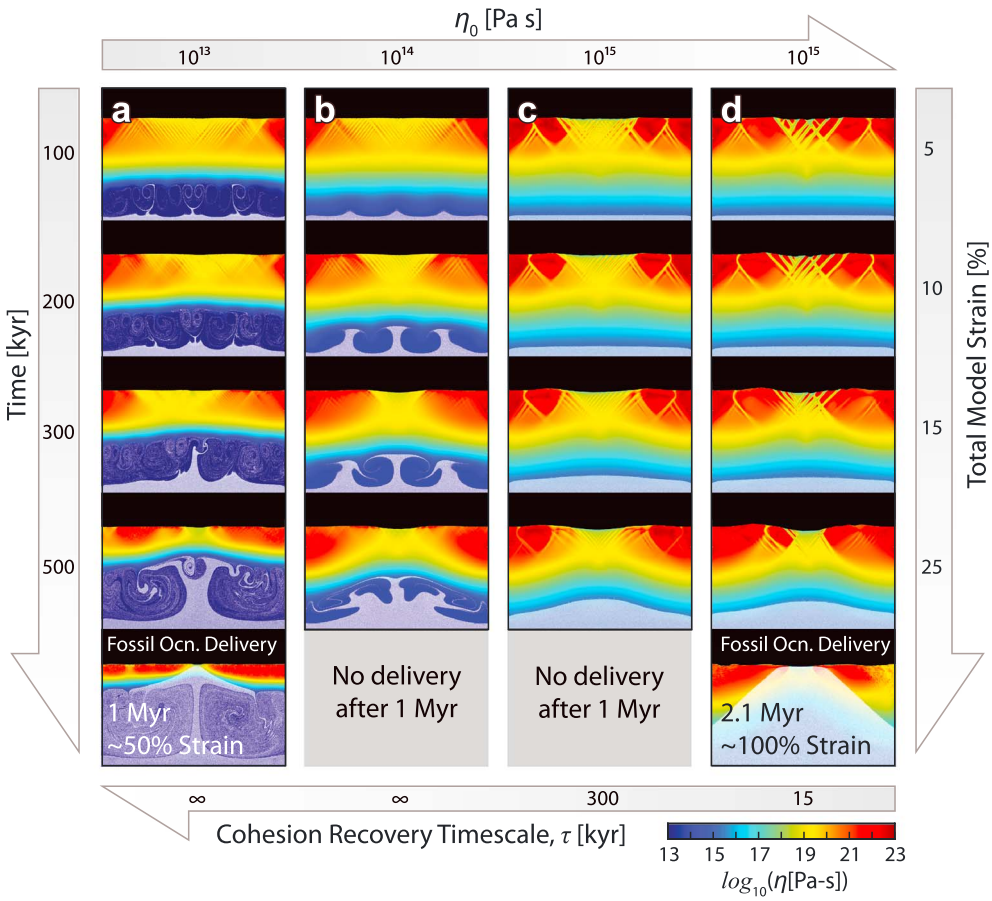

Figure 3. Selected models illustrating the spectrum of band evolution and morphology, controlled by lithosphere strength. Models show that (a) low viscosity and poor localization produces broad yielding. With increasing η_0 (b) and decreasing τ (c), broad yielding gives way to closely grouped tectonic shear bands. For the highest η_0 and lowest τ (d), rifting processes dominate at all but the highest strains.

At low strains, a highly convective ice shell with no fault healing ($\eta_0 = 1 \times 10^{13}$ Pa·s, $\tau = \infty$) exhibits broad yielding when initially undamaged (Figure 4a) and more focused yielding when preweakened (Figure 4b). At higher strains and with greater thinning of the lithosphere, a significant fraction of the lithosphere (upper ~1 km) is under absolute tension. The initially undamaged lithosphere produces a smooth zone of frictional plastic yielding, while the preweakened lithosphere bends elastically to "zipper" open along the weakened column. This produces a discrete margin between newly exposed ice at the band and the surrounding older terrain.

At low strains, a weakness imposed within a purely conductive ice shell with rapid fault healing ($\eta_0 = 1 \times 10^{15}$ Pa·s, $\tau = 15$ kyr) has little effect on the tectonic structure (Figures 4c and 4d). At higher stains and without vigorous convection, a much smaller fraction of the lithosphere is under tension than in the convecting case, and the vertical column is at an energetically unfavorable orientation to accommodate motion (Anderson, 1951). If the imposed weakness rotates nearer to the angle of fault initiation predicted by Anderson-Byerlee theory (~60°), then it may facilitate formation of a through-going normal fault that accommodates significant extension.

4.3. Implications for Observed Morphologies

For comparison with the principal band types identified on Europa and Ganymede, we present output from the full range of model results that are most similar to the presented band observations (Figure 1).

4.3.1. Smooth Bands

A weak lithosphere reproduces the features observed at Europa's smooth bands (Figure 1e). A low η_0 (10^{13} Pa·s) promotes vigorous convection that thins and weakens the lithosphere in a 25 km thick ice shell,

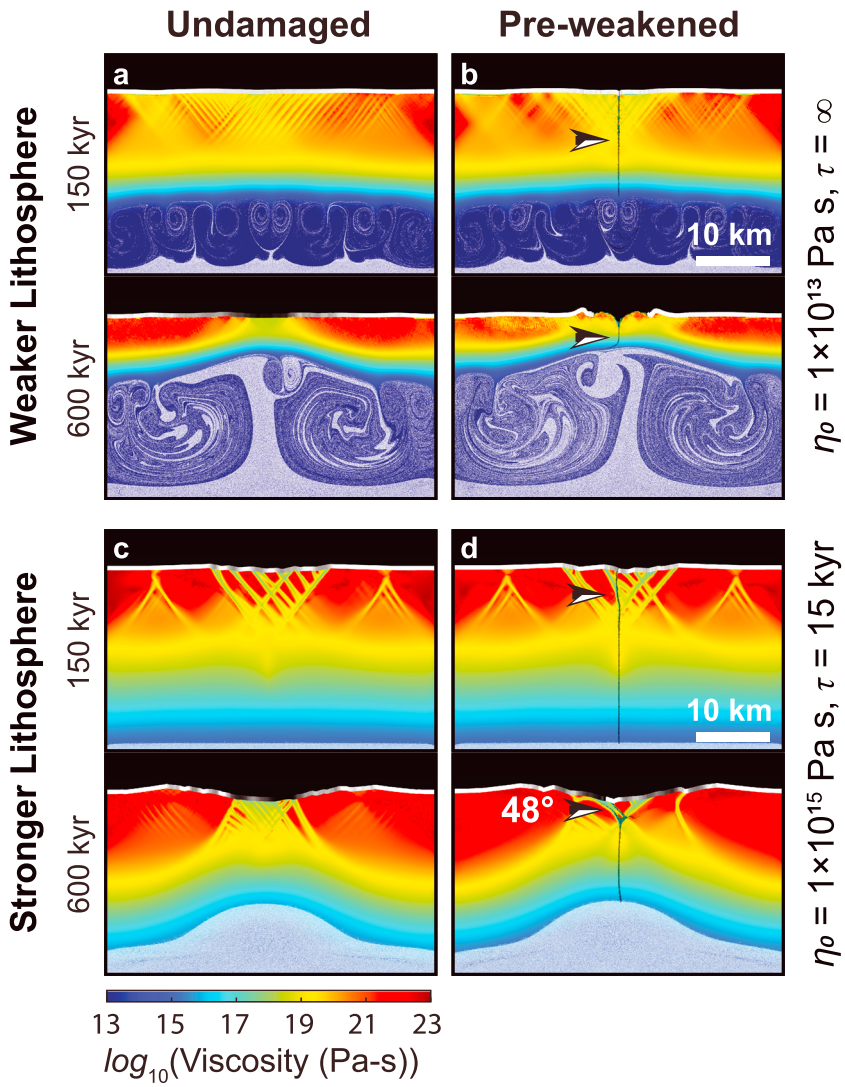

Figure 4. Models showing the effect of a preexisting vertical weakness on band evolution. The top panels show two different time steps for models of $\eta_0 = 10^{13}$ Pa·s, $\tau = \infty$, (a) H = 25 km and (b) 50 km, with and without an imposed weakness (black lines marked by arrows).

resulting in a relatively high lithosphere thermal gradient of 20–30 K/km at the axis. Moreover, poorly localized failure ($\tau = \infty$) results in a broadly weakened, low-cohesion lithosphere, where passive upwelling responding to the diverging ice shell promotes exposure of fresh ice above the central zone of yielding, beginning at the band center. After 20 km total extension, a topographically smooth band has exposed new ice across approximately the total opening width, exhibiting <100 m tectonic topography and a 2 km wide, 200 m deep central depression (Figure 4b). These topographic amplitudes are consistent with observations of Europa band topography (Nimmo et al., 2003).

An alternate explanation for the origin of smooth bands consistent with observations of sharp band margins comes from models that consider a preexisting vertical weakness through the ice shell (Figure 4b). Thin lithosphere opens along a weakened column and "unzips" outward away from the band center, producing well-defined margins. Whether due to yielding of weak lithosphere or separation along a preexisting vertical weakness, smooth bands form only in thin lithosphere above vigorously convecting ductile ice.

4.3.2. Lineated Bands

A moderately weak lithosphere reproduces features observed at lineated bands (Figure 1f). A moderate η_0 (10^{14} Pa·s) allows deep-seated convection to slowly thin the lithosphere in a 25-km thick ice shell. After 10 km total extension, the axial lithosphere thins and produces an axial thermal gradient of 5–15 K/km.

Variations in lithosphere strain rate produce small variations in surface ice exposure at the axis, though the band remains relatively topographically smooth, exhibiting <100 m tectonic topography superimposed on ~ 600 m of flexural topography.

4.3.3. Ridged Bands

A moderately strong lithosphere reproduces characteristics of ridged bands after 5 km extension (Figure 1g). A moderate η_0 (10^{14} Pa·s) and short cohesion recovery timescale (τ = 15 kyr) produce an axial heat flow of 3–12 K/km and ensure that deformation is well localized. Many simultaneously active faults disrupt the surface over ~15 km with no distinct central axis of opening. These faults exhibit ~2.5 km spacing and up to 500 m relief, preventing subsequent reconstruction of the deformed terrain. The highly tectonized surface may undergo additional fracturing and/or diking that shape the terrain.

4.3.4. Groove Lanes and Rifted Terrains

A very strong lithosphere reproduces features observed at Ganymede's groove lanes after only 1 km extension (Figure 1h). A 50-km-thick ice shell retains a nearly conductive temperature profile because the high η_0 (10^{15} Pa·s) inhibits convection, despite our assumed overestimate of tidal heat input for Ganymede. Deformation is well localized (τ = 15 kyr), and widespread faulting tectonically disrupts the surface over a region nearly 40 km wide. Faults exhibit ~300 m relief and spacing of ~5 km. With a small increase in strain, large-scale rifting occurs. A highly tectonized band begins to form with a lithosphere thermal gradient of only 3–4 K/km (model shown in Figure 1h), consistent with the estimates of groove terrain formation by Kirk and Stevenson (1987) but less than the >10 K/km required by Dombard and McKinnon (2001) to explain the long tectonic wavelengths observed within grooved terrain.

Our models indeed predict that the lithosphere thins and weakens at high heat flows to form a long-wavelength necking instability. However, such high heat flows result in convective thinning of the lithosphere that inhibits formation of shorter wavelength tectonic structures associated with localized faulting. In all cases, our modeled heat flow is imposed through the assumptions of constant ice shell thickness, surface temperature, and melting temperature viscosity. Thus, to fully explore the possible role of necking instability in creating constituent structures, further studies should consider the full applicable range of these parameters and their variation across Ganymede spatially and through time.

Our models predict that rifted band formation occurs in response to ~2–10% regional strain. At strains >10%, faults give way to broad yielding that produces little topography. The resulting morphology is that of a smooth band nested within a highly tectonized band, which is not widely observed on Ganymede. Some estimates of groove lane strain inferred through strained crater and surface mapping can exceed 100% (Collins et al., 1998; Pappalardo & Collins, 2005), but as noted by Bland and McKinnon (2015), modest regional strains are not inconsistent with large strains across individual features.

5. Conclusions

From numerical simulations of ice I under extension, we infer that bands observed on Europa and Ganymede occupy a spectrum of morphologies controlled by the strength of the lithosphere. Where the lithosphere is weak, that is, thin and/or with broadly lowered cohesion, smooth bands with central axes can form at high strains and may exploit preexisting weaknesses to produce sharp band margins. For stronger lithosphere, that is, thicker and with deformation localized onto few discrete faults, tens of kilometers of ice shell surface may be tectonically disrupted after only a few kilometers of extension. Europa's bands may form at relatively high regional strains and high lithosphere thermal gradients, and groove lanes on Ganymede may form at relatively low strains and small thermal gradients.

Models of thick, conductive ice shells produce rifted terrains that resemble ridged bands and groove lanes only at low strains. In these models, fossil ocean material is exposed only after a total extension of 40 km (Europa) to 80 km (Ganymede). The resulting model bands exhibit smooth terrains bounded by highly tectonized terrains, which are not prevalent on the surfaces of these bodies. Because small strains and thick lithosphere are required, rifted terrains are unlikely to expose fossil ocean material or facilitate ocean-surface interaction on Europa and Ganymede. Thus, spacecraft are unlikely to contaminate potential ocean material by contacting such regions, notably at Ganymede's groove lanes.

In models that simulate a vigorously convecting ductile ice interior, rapid convective transport can quickly deliver fossil ocean material to the base of the lithosphere. For Europa, lithosphere thinned by convection

and mechanical stretching permits surface exposure of fossil ocean material along the center of a topographically smooth band after ~20 km of extension. The timescale of delivery, which depends on the band opening rate, is ~1 Myr in these models. Therefore, currently planned and potential future spacecraft missions to study Europa should consider the center swaths of the widest smooth and lineated bands as the tectonic sites most likely to expose fossil ocean material.

Acknowledgments
This work was supported by NASA through the Europa Clipper project. This research was carried out at the Jet Propulsion Laboratory, California Institute of Technology, under contract with the National Aeronautics and Space Administration. No new data were used in producing this manuscript. We thank J.-A. Olive, E. Mittelstaedt, B. Klein, M. Behn, and G. Ito for developing and supporting SiStER and J.-A. Olive and M. E. Cameron for informally reviewing an early draft of this manuscript. We further thank W. R. Buck for his formal review of this manuscript.

References

Anderson, E. M. (1951). *The dynamics of faulting and dyke formation with applications to Britain* (2nd ed.). Edinburgh: Oliver and Boyd.
Behn, M. D., & Ito, G. (2008). Magmatic and tectonic extension at mid-ocean ridges: 1. Controls on fault characteristics. *Geochemistry, Geophysics, Geosystems*, *9*, Q08O10. https://doi.org/10.1029/2008GC001965
Bland, M. T., & McKinnon, W. B. (2015). Forming Ganymede's grooves at smaller strain: Toward a self-consistent local and global strain history for Ganymede. *Icarus*, *245*, 247–262. https://doi.org/10.1016/j.icarus.2014.09.008
Buck, W. R., Lavier, L. L., & Poliakov, A. N. (2005). Modes of faulting at mid-ocean ridges. *Nature*, *434*(7034), 719–723. https://doi.org/10.1038/nature03358
Collins, G. C., Head, J. W., & Pappalardo, R. T. (1998). Formation of Ganymede Grooved Terrain by Sequential Extensional Episodes: Implications of Galileo Observations for Regional Stratigraphy. *Icarus*, *135*(1), 345–359. https://doi.org/10.1006/icar.1998.5978
Dombard, A. J., & McKinnon, W. B. (2001). Formation of Grooved Terrain on Ganymede: Extensional Instability Mediated by Cold, Superplastic Creep. *Icarus*, *154*(2), 321–336. https://doi.org/10.1006/icar.2001.6728
Goldsby, D. L., & Kohlstedt, D. L. (2001). Superplastic deformation of ice: Experimental observations. *Journal of Geophysical Research*, *106*(B6), 11017–11030. https://doi.org/10.1029/2000JB900336
Grasset, O., Bunce, E. J., Coustenis, A., Dougherty, M. K., Erd, C., Hussmann, H., et al. (2013). Review of exchange processes on Ganymede in view of its planetary protection categorization. *Astrobiology*, *13*(10), 991–1004. https://doi.org/10.1089/ast.2013.1013
Hand, K. P., Chyba, C. F., Priscu, J. C., Carlson, R. W., & Nealson, K. H. (2009). Astrobiology and the potential for life on Europa. In R. T. Pappalardo, W. B. McKinnon, & K. Khurana (Eds.), *Europa* (Part V, pp. 589–629). Tucson: University of Arizona Press.
Head, J. W., Pappalardo, R. T., & Sullivan, R. (1999). Europa: Morphological characteristics of ridges and triple bands from Galileo data (E4 and E6) and assessment of a linear diapirism model. *Journal of Geophysical Research*, *104*(E10), 24,223–24,236. https://doi.org/10.1029/1998JE001011
Howell, S. M., Ito, G., Behn, M. D., Martinez, F., Olive, J.-A., & Escartín, J. (2016). Magmatic and tectonic extension at the Chile Ridge: Evidence for mantle controls on ridge segmentation. *Geochemistry, Geophysics, Geosystems*, *17*, 2354–2373. https://doi.org/10.1002/2016GC006380
Johnson, B. C., Sheppard, R. Y., Pascuzzo, A. C., Fisher, E. A., & Wiggins, S. E. (2017). Porosity and salt content determine if subduction can occur in Europa's ice shell. *Journal of Geophysical Research: Planets*, *122*, 2765–2778. https://doi.org/10.1002/2017JE005370
Kalousová, K., Souček, O., Tobie, G., Choblet, G., & Čadek, O. (2016). Water generation and transport below Europa's strike-slip faults. *Journal of Geophysical Research: Planets*, *121*, 2444–2462. https://doi.org/10.1002/2016JE005188
Kattenhorn, S. A., & Hurford, T. A. (2009). Tectonics of Europa. In R. T. Pappalardo, W. B. McKinnon, & K. Khurana (Eds.), *Europa* (pp. 199–236). Tuscon: University of Arizona Press.
Kattenhorn, S. A., & Prockter, L. M. (2014). Evidence for subduction in the ice shell of Europa. *Nature Geoscience*, *7*(10), 762–767. https://doi.org/10.1038/ngeo2245
Kirk, R. L., & Stevenson, D. J. (1987). Thermal evolution of a differentiated Ganymede and implications for surface features. *Icarus*, *69*, 91–134. https://doi.org/10.1016/0019-1035(87)90009-1
Mitri, G., & Showman, A. P. (2005). Convective–conductive transitions and sensitivity of a convecting ice shell to perturbations in heat flux and tidal-heating rate: Implications for Europa. *Icarus*, *177*(2), 447–460. https://doi.org/10.1016/j.icarus.2005.03.019
Nimmo, F., Giese, B., & Pappalardo, R. T. (2003). Estimates of Europa's ice shell thickness from elastically-supported topography. *Geophysical Research Letters*, *30*(5), 1233. https://doi.org/10.1029/2002GL016660
Nimmo, F., & Manga, M. (2009). Geodynamics of Europa's icy shell. In R. T. Pappalardo, W. B. McKinnon, & K. Khurana (Eds.), *Europa* (Part III, pp. 381–404). Tucson: University of Arizona Press.
Olive, J.-A., Behn, M. D., Ito, G., Buck, W. R., Escartín, J., & Howell, S. (2015). Sensitivity of seafloor bathymetry to climate-driven fluctuations in mid-ocean ridge magma supply. *Science*, *350*(6258), 310–313. https://doi.org/10.1126/science.aad0715
Olive, J.-A., Behn, M. D., Mittelstaedt, E., Ito, G., & Klein, B. Z. (2016). The role of elasticity in simulating long-term tectonic extension. *Geophysical Journal International*, *205*(2), 728–743. https://doi.org/10.1093/gji/ggw044
Pappalardo, R. T., & Collins, G. C. (2005). Strained craters on Ganymede. *Journal of Structural Geology*, *27*(5), 827–838. https://doi.org/10.1016/j.jsg.2004.11.010
Pappalardo, R. T., Collins, G. C., Head, J. W., Helfenstein, P., McCord, T. B., Moore, J. M., et al. (2004). Geology of Ganymede. In F. D. Bagenal, T. E. Dowling, & W. B. McKinnon (Eds.), *Jupiter* (pp. 363–396). Cambridge, UK: Cambridge University Press.
Pappalardo, R. T., Head, J. W., Collins, G. C., Kirk, R. L., Neukum, G., Oberst, J., et al. (1998). Grooved terrain on Ganymede: First results from Galileo high-resolution imaging. *Icarus*, *135*(1), 276–302. https://doi.org/10.1006/icar.1998.5966
Pizzi, A., Domenica, A. D., Komatsu, G., Cofano, A., Mitri, G., & Bruzzone, L. (2017). Spreading vs. rifting as modes of extensional tectonics on the globally expanded Ganymede. *Icarus*, *288*, 148–159. https://doi.org/10.1016/j.icarus.2017.01.034
Poliakov, A. N. B., & Buck, W. R. (1998). Mechanics of stretching elastic-plastic-viscous layers: Applications to slow-spreading mid-ocean ridges. In *Faulting and magmatism at mid-ocean ridges* (pp. 305–323). Washington, DC: American Geophysical Union.
Prockter, L. M., Head, J. W., Pappalardo, R. T., Sullivan, R. J., Clifton, A. E., Giese, B., et al. (2002). Morphology of Europan bands at high resolution: A mid-ocean ridge-type rift mechanism. *Journal of Geophysical Research*, *107*(E5), 5028. https://doi.org/10.1029/2000JE001458
Prockter, L. M., & Patterson, G. W. (2009). Morphology and evolution of Europa's ridges and bands. In R. T. Pappalardo, W. B. McKinnon, & K. Khurana (Eds.), *Europa* (Part II, pp. 237–258). Tucson: University of Arizona Press.
Schenk, P. M., McKinnon, W. B., Gwynn, D., & Moore, J. M. (2001). Flooding of Ganymede's bright terrains by low-viscosity water-ice lavas. *Nature*, *410*(6824), 57–60. https://doi.org/10.1038/35065027
Showman, A. P., & Han, L. (2004). Numerical simulations of convection in Europa's ice shell: Implications for surface features. *Journal of Geophysical Research*, *109*, E01010. https://doi.org/10.1029/2003JE002103
Spohn, T., & Schubert, G. (2003). Oceans in the icy Galilean satellites of Jupiter? *Icarus*, *161*(2), 456–467. https://doi.org/10.1016/S0019-1035(02)00048-9

Stempel, M. M., Barr, A. C., & Pappalardo, R. T. (2005). Model constraints on the opening rates of bands on Europa. *Icarus*, *177*(2), 297–304. https://doi.org/10.1016/j.icarus.2005.03.025

Tian, X., & Choi, E. (2017). Effects of axially variable diking rates on faulting at slow spreading mid-ocean ridges. *Earth and Planetary Science Letters*, *458*, 14–21.

Zahnle, K., Schenk, P., Levison, H., & Dones, L. (2003). Cratering rates in the outer solar system. *Icarus*, *163*(2), 263–289. https://doi.org/10.1016/S0019-1035(03)00048-4

Erratum

In the originally published version of this article, temperature gradients were erroneously reported in km/K rather than in K/km. This correction has been made, and the present version may be considered the authoritative version of record.